

Published in final edited form as:

Biomaterials. 2013 August ; 34(26): 6133–6138. doi:10.1016/j.biomaterials.2013.04.051.

Combinatorial synthesis with high throughput discovery of protein-resistant membrane surfaces

Minghao Gu^a, Arturo J. Vegas^b, Daniel G. Anderson^b, Robert S. Langer^b, James E. Kilduff^c, and Georges Belfort^{a,*}

^aHoward P. Isermann Department of Chemical and Biological Engineering and Center for Biotechnology and Interdisciplinary Studies, Rensselaer Polytechnic Institute, Troy, NY 12180-3590, USA

^bDepartment of Chemical Engineering, Division of Health Science and Technology, David H. Koch Institute for Integrative Cancer Research, Massachusetts Institute of Technology, Cambridge, MA 02139, USA

^cDepartment of Civil and Environmental Engineering, Rensselaer Polytechnic Institute, Troy, NY 12180-3590, USA

Abstract

Using combinatorial methods, we synthesized a series of new vinyl amide monomers and graft-polymerized them to light-sensitive poly(ether sulfone) (PES) porous films for protein resistance. To increase the discovery rate and statistical confidence, we developed high throughput surface modification methods (HTP) that allow synthesis, screening and selection of desirable monomers from a large library in a relatively short time (days). A series of amide monomers were synthesized by amidation of methacryloyl chloride with amines and grafted onto commercial poly(ether sulfone) (PES) membranes using irradiation from atmospheric pressure plasma (APP). The modified PES membrane surfaces were then tested and screened for static protein adhesion using HTP. Hydroxyl amide monomers N-(3-hydroxypropyl)methacrylamide (A3), N-(4-hydroxybutyl)methacrylamide (A4), and N-(4-hydroxybutyl) methacrylamide (A6), ethylene glycol (EG) monomer N-(3-methoxypropyl)methacrylamide (A7), and N-(2-(dimethylamino)ethyl)-N-methylmethacrylamide (A8), and N-(2-(diethylamino)ethyl)-N-methylmethacrylamide (A9) all terminated with tertiary amines and were shown to have protein resistance. The PES membranes modified with these monomers exhibited both low protein adhesion (i.e. membrane plugging or fouling) and high flux. Their performance is comparable with previously identified best performing PEG and zwitterionic monomers, i.e. the so-called gold-standard for protein resistance. Combining a Hansen solubility parameter (HSP) analysis of the amide monomers and the HTP filtration results, we conclude that monomer solubility in water correlates with protein-resistant surfaces, presumably through its effects on surface–water interactions.

Keywords

Low protein adhesion; Combinatorial chemistry; Amide monomer; High throughput; Atmospheric pressure plasma

*Corresponding author. Tel.: +1 518 276 6948. belfog@rpi.edu (G. Belfort).

Appendix A. Supplementary data

Supplementary data related to this article can be found at <http://dx.doi.org/10.1016/j.biomaterials.2013.04.051>.

1. Introduction

Nonspecific protein adsorption on surfaces has a significant negative effect on the performance of materials as drug delivery [1], implantable medical device and biosensors [2] and synthetic membrane filtration application (cite) [3,4]. Whitesides have developed criteria for protein resistance with four molecular characteristics: surfaces should (i) be hydrophilic (high wettability), (ii) incorporate hydrogen bond acceptors, (iii) not include hydrogen bond donors, and (iv) be net electrically neutral [5,6]. Examples include self-assembled monolayers (SAMs) of oligo(ethylene glycol) (OEG), tertiary amines, zwitterionics and combination of positively charged and negatively charged moieties [7–9]. The exception to Whitesides criteria is sugar-based SAMs with multiple hydroxyl functional groups that possess hydrogen bond donors [5,10].

To date few non-fouling materials have been discovered over the past 30 years. Polyethylene glycol (PEG) meets the above criteria and has been widely used for biomedical applications [11,12]. However, PEG-based materials have limitations since they decompose in the presence of oxygen and transition metal ions [13]. To overcome this limitation, zwitterionic polymers or polyampholytes constructed with charge balance of positively and negatively charged monomers have been developed [5]. They exhibit comparable non-fouling characteristics comparable to PEG but also more stable [7,8,14]. Non-fouling materials also have been developed by tailoring existing material surfaces with functional polymer chains. This approach does not substantially alter the bulk material properties, but enhance the wetting, charge, dyeing, adhesion or non-fouling properties of these materials [15–19].

Fouling is a significant challenge for membrane filtration since it diminishes the separation capabilities and increases the cost for membrane cleaning and replacement. Fouling is caused by accumulation, deposition and adsorption of particles, colloids or biological molecules on the membrane surface (external fouling) or within membrane pores (internal fouling) [3]. Researchers have focused on the surface modification of synthetic membranes using graft polymerization to reduce fouling [20–23]. However, only a few low fouling membranes have been discovered over the past 30 years. Previously, we described a high throughput platform (HTP) combined with a photo-grafting method that facilitated quick synthesis and screening of protein-resistant membrane surfaces from a library of commercial vinyl monomers [24–27]. Membrane surfaces grafted with hydroxyl, PEG, amine and zwitterionic monomers exhibited protein resistance. Moreover, based on these HTP results, the mechanism of non-fouling has also been investigated with the help of structure–property relationships [26]. As the number of the commercially available vinyl monomers is limited, there are opportunities to expand this library approach, increase the variety of protein-resistant surfaces, and explore protein adhesion or fouling mechanisms.

Here we develop combinatorial methods for acquiring protein-resistant surfaces [23–28]. Related approaches have been utilized to rapidly synthesize a library of molecules and materials, such as catalysts [28], enzymes inhibitors [29], protein receptors [30], peptide ligands [31], and polymers [32]. To this end, we synthesized ten amide monomers by amination of methacryloyl chloride with amine compounds (Fig. 1) and confirmed their target masses with mass spectrometry (Figs. S1–S10). The amide monomers were functionalized with alkane (A1), bis-amide (A2), hydroxyl (A3–A6), ethylene glycol amine (A7), tertiary amine (A8, A9) and morpholino amine (A10) groups. Combined with the HTP method, these monomers were rapidly graft polymerized onto poly(ethersulfone) (PES) ultrafiltration membrane surfaces using atmospheric pressure plasma (APP) [26]. The anti-fouling performance of these modified membranes was evaluated with a static protein adsorption assay and the results were correlated with Hansen solubility parameters (HSPs).

2. Experimental

2.1. Materials

Amylamine (99%), 1,4-diaminobutane (99.0%, GC grade), 3-amino-1-propanol (99.0%), 4-amino-1-butanol (98%), 6-amino-1-hexanol (97%), 2-amino-1-butanol (97%), 3-methoxypropylamine (99%), N,N,N'-trimethyl-ethylenediamine (97%), N,N-diethyl-N'-methylethylenediamine (97%), 4-(2-aminoethyl)morpholine (99%), dichloromethane (DCM, 99.9%, HPLC grade), N,N-diisopropylethylamine (DIPEA, 99.5%, biotech grade), hexane (95%, HPLC grade), ethyl acetate (EtOAc, 99.9%, HPLC grade), ethanol (99.5%), and sodium chloride (95%) were purchased from Sigma Aldrich (St. Louis, MO), which were used without further purification. 96-well filter plates (CMR# 1746-3, Seahorse Labware, Chicopee, MA) were used for the HTP grafting and filtration. Silica Gel (230–400 Mesh, Grade 60) was purchased from Fisher Scientific (Pittsburg, PA). Magnesium sulfate powder (99.5%, anhydrous) was purchased from Alfa Aesar (Ward Hill, MA). PES membranes (100 kDa) having an effective area of 19.95mm² were mounted and sealed by the manufacturer (Seahorse Bioscience, North Billerica, MA) on the bottom of each well of a 96-well plate (volume of 300 μ L). The membranes were washed and soaked in DI water overnight before use to remove surfactant. Ultrahigh purity helium gas was used as a plasma source (Noble Gas Solutions, Albany, NY). Solution for the static protein adsorption assay was prepared by dissolving 1 mg/mL bovine serum albumin (BSA, molecular weight (MW) 67 kDa, pI 4.7) in 200 mL phosphate buffered saline (PBS) solution. BSA and PBS tablets were purchased from Sigma Aldrich (St. Louis, MO). When dissolved in 200mL of water, a PBS tablet yields 10 mmol L⁻¹ phosphate buffer, 2.7 mmol L⁻¹ potassium chloride and 137 mmol L⁻¹ sodium chloride with pH 7.4 at 25 °C.

2.2. Methods

2.2.1. Monomer synthesis—Amine (1 mmol), and DIPEA (3 mmol) were first added to DCM (4 mL), and then an abundant amount of methacryloyl chloride (1.5 mmol) was added. The mixture was stirred for 0.5 h at 0 °C for 2 h at room temperature and under a nitrogen blanket. The crude products were first washed by extraction with brine twice, and the organic phase was collected which was then concentrated by evaporation at room temperature under vacuum (VWR 1410, VWR, Radnor, PA). The resultant residue was purified by column chromatography on a silica gel column (EtOAc/hexane, 50% vol/50% vol), concentrated by evaporation at room temperature under vacuum oven, and dried with magnesium sulfate under vacuum desiccator (VWR[®] Desi-Vac[™], WR, Radnor, PA) overnight.

2.2.2. HTP-APP—Membranes located at the base of each well in the 96 filter plate were, first exposed to an atmospheric pressure (AP) plasma source (Model ATOMFLO, Surfex Technologies LLC, Culver City, CA) at a helium flow rate of 30.0 L min⁻¹ and a source-to-membrane distance of 13mm (Fig. S11). The plasma source was operated at 200 V and driven by a radio frequency power at 27.12 MHz. An XYZ Robot (Surfex Technologies LLC, Culver City, CA) was used to control the plasma source over the plate with a scan speed of 0.7 mm s⁻¹. Following exposure to the plasma and subsequent formation of radicals at the membrane surface, 200 μ L of monomer solution was added to each well in the filter plate. Graft polymerization was immediately initiated at 60 \pm 1 °C for 2 h. The reaction was terminated by adding DI water. The 96 membranes in the filter plate were then soaked and rinsed with DI water for 24 h to remove any homopolymer and unreacted monomer residue from the membranes surfaces [33].

2.2.3. Assay for protein adhesion: high throughput filtration and evaluation—Filtration of protein solution in a 96-well filter plate was performed on a multi-well plate

vacuum manifold (Pall Corp., Port Washington, NY) at a constant transmembrane pressure (TMP) of 68 kPa and $T = 22 \pm 1$ °C. The permeate was collected in an acrylic 96-well receiver plate (Corning Inc., Corning, NY) placed under the 96-well filter plate establishing well-to-well alignment. The volume of permeate in each receiver well was calculated by measuring the absorbance at 977nm of permeate solution in the receiver plate wells using a Microplate Spectrophotometer (PowerWave XS, BioTek Instruments Inc., Winooski, VT). Permeation flux, J_v (m s^{-1}), is defined as $J_v = V/(At)$, where V (m^3) is the cumulative volume of permeate, A (m^2) is the membrane surface area, and t (s) is the filtration time. Membrane resistance is defined as $R = \Delta P/(\mu J_v)$, where ΔP (Pa) is TMP and μ ($\text{gm}^{-1} \text{s}^{-1}$) is the solution viscosity. The volume of permeate in each receiver well was calculated by measuring the absorbance at 977nm of permeate solution in the receiver plate wells using a Microplate Spectrophotometer (PowerWave XS, BioTek Instruments Inc., Winooski, VT).

The protein adhesion and subsequent pore blocking (i.e. anti-fouling performance) was measured in terms of a fouling index, \mathcal{R} (Fig. S12):

$$\mathcal{R} = [(R_{\text{fouled}} - R_{\text{PBS}})_{\text{mod}} / (R_{\text{fouled}} - R_{\text{PBS}})_{\text{control}}] \quad (1)$$

Here, $R_{\text{PBS,mod}}$ and $R_{\text{PBS,control}}$ are resistances to the PBS flux for the modified and unmodified membranes before BSA fouling, respectively. $R_{\text{fouled,mod}}$ and $R_{\text{fouled,control}}$ are resistances to the PBS flux for the modified and unmodified membranes after BSA fouling, respectively. \mathcal{R} is defined as the ratio of the increase in resistance due to BSA fouling of the control or unmodified membrane due to BSA fouling. $\mathcal{R} < 1$ indicates that the modified membranes exhibited less BSA fouling than the control or unmodified membrane.

Membrane selectivity was measured after filtration with 1 mg/mL BSA solution (*dynamic fouling*) and is defined as.

$$\psi = C_b / C_p \quad (2)$$

where C_b and C_p are the BSA concentration in the feed and permeate, respectively. The BSA concentration in the permeate was calculated by measuring the absorbance (at 280 nm) of permeate solution in the receiver plate wells.

2.2.4. Hansen solubility parameters characterization—Surface properties of PES membrane surfaces were characterized using Hansen solubility parameters (HSPs). HSPs are defined as the square root of the cohesive energy density and used to characterize the physical properties of the modified surfaces [34]. HSPs consist of three components (i) “non-polar” or dispersion interactions (δ_d), (ii) “polar” or permanent dipole–permanent dipole interactions (δ_p), and (iii) hydrogen bonding interactions (δ_h). Each component is estimated from the molecular physical properties of each molecular group in a monomer. This is a group contribution method [26,35], where

$$\delta_d = \left(\sum F_d \right) / V \quad (3)$$

$$\delta_p = \left(\sum F_p^2 \right)^{1/2} / V \quad (4)$$

$$\delta_h = \left(\sum U_h / V \right)^{1/2} \quad (5)$$

where F_d ($J^{1/2} \text{ cm}^{2/3} \text{ mol}^{-1}$), F_p ($J^{1/2} \text{ cm}^{2/3} \text{ mol}^{-1}$) and U_h ($J \text{ mol}^{-1}$) are the molar attraction constant for the non-polar groups, the molar attraction constant for the polar group and the hydrogen bonding energy, respectively. V ($\text{cm}^3 \text{ mol}^{-1}$) is the monomer molar volume.

3. Results and discussion

3.1. Protein adhesion (anti-fouling) performance of modified PES membranes

In Fig. 2, PES membrane surfaces grafted with low water soluble amide monomers A1, A2, and A5 exhibited $\mathcal{R} > 1$, which means that BSA fouled these modified surfaces to a greater extent than the control membrane surface. \mathcal{R} values for A1 and A2 modified membrane surfaces did not show a dependence on monomer concentration, whereas \mathcal{R} values for A5 modified membranes increased when the concentration of A5 increased from 0.1 to 0.2 M, reaching the highest $\mathcal{R} = 1.65 \pm 0.06$ after grafting with 0.2 M. The finding that $\mathcal{R} > 1$ for membranes modified with A1 and A5 was anticipated, as they comprise six units of repeated hydrophobic alkane groups. An increase in fouling index with concentration is consistent with an increase in the degree of grafting (DG), which would result in higher BSA adsorption on the membrane surface. The lack of such an effect for A1 is likely due to the low degree of grafting, even at high monomer concentrations.

Membranes modified with water-soluble amide monomers A3, A4, and A6–A9, exhibited lower BSA fouling than the control membrane surface (A10 was an exception). Membranes modified with monomer A7 at a concentration of 0.3 M had the lowest value of $\mathcal{R} = 0.58 \pm 0.01$. \mathcal{R} values for membranes modified with monomers A3, A4 and A7 decreased with increasing monomer concentration and DG. Hydroxyl terminated monomers A3–A6 had similar chemical structure; however, membranes modified with monomer A5 exhibited a higher \mathcal{R} value than those modified with A3, A4 and A6. Though \mathcal{R} values did not have the expected dependence on the length of the alkane groups, the A5 monomer had the longest alkyl chain length (six units of repeated alkane groups) and the highest \mathcal{R} value, suggesting that there may be a maximum chain length for hydroxyl amide methacrylates, above which $\mathcal{R} > 1$. Tertiary amide monomers A8 and A9 showed comparable protein adhesion (antifouling) to hydroxyl amide monomers A3, A4 and A6 and did not exhibit monomer concentration dependency.

3.2. Surface characterization with Hansen solubility parameters

Empirical and modeling studies have determined that protein resistance is mainly due to surface–water interactions that prevent a protein's approach to a surface [11,36–38]. Hower et al. [39] quantified protein resistance of a surface by evaluating the intrinsic hydration capacity of different chemical groups (ethylene glycols, sugar alcohols, and glycine analogs). Here, the Hansen solubility parameters (HSPs) are used to quantify the grafted surface–water interactions by assuming that the properties of the monomers sufficiently represent the interactive properties of the grafted polymers. Non-polar (δ_d), polar (δ_p), and hydrogen-bonding (δ_h) components of the HSPs for monomers A1–A10 were estimated using a group contribution method [35]. δ_d versus $(\delta_p^2 + \delta_h^2)^{1/2}$ for the interaction of each monomer with water is plotted in Fig. 3. The distance from the water point is considered as a measure of water affinity (dashed circles are to help guide the eye). Monomers A1 and A2 were further away from the water coordinate than the other amide monomers. This indicates weaker interactions between A1 and A2 modified surfaces with water, which is consistent with their higher \mathcal{R} values (Fig. 2). As the length of the alkane chain increases from A3 to A5, the distance from the water coordinate also increases. Therefore, the lower \mathcal{R} values for membranes modified with monomers A3 and A4 compared to those modified with A5 could be attributed to stronger interactions between the water and the modified surface. Oligo(ethylene glycol) amide monomer A7 showed weak interactions with the water, but

membranes modified with this monomer still had $\mathcal{R} < 1$. This is consistent with our previous findings in which PEG monomers (#s 6–12 [26]) exhibited relatively weak interactions with water but PEG-modified membranes still gave $\mathcal{R} < 1$ [26]. It suggests that protein resistance for PEG or OEG grafted surfaces is not only due to strong interactions with water, but is also determined by the flexible helical conformation of PEG or OEG which facilitates formation of a tight hydration layer [11,36,37,40]. In Fig. 4, the fouling index, \mathcal{R} , of the modified surfaces at 0.3 M monomer concentration (Fig. 2) is plotted against the distance, d_{M-H_2O} , between a monomer point and the water point in Fig. 3. Their correlation suggests that a monomer highly soluble in water (smaller value of d_{M-H_2O}), will result in lower protein fouling. Hence water–interface interactions are important.

3.3. Development of protein-resistant membranes

Protein-resistant membranes require both low fouling (\mathcal{R} , or protein adhesion) and high permeation (or low resistance to flow through the membrane). Here, the ratio of the resistance to flow of the modified membrane to that of the control, or the ratio of the inverse PBS fluxes, is plotted against fouling index, \mathcal{R} (Fig. 5). Desirable performance is in the direction of the arrow or toward the origin. Data for three additional membranes are included for reference: an unmodified membrane (control), as well as PEG(#8) and zwitterionic (#40) modified membranes from earlier work [22]. PES membrane modified with monomers A8 and A9 displayed lower \mathcal{R} values than the control membrane (as in Fig. 2), but also had higher resistance. In contrast, A3, A4 and A7 modified PES membranes gave both lower \mathcal{R} values and higher flux than the control membrane. Surfaces modified with monomer A7 had slightly lower fluxes but similar \mathcal{R} values to those modified with monomer A4 as expected (Fig. 3). Monomers A4 and A7 yielded surfaces having comparable filtration performance with those modified with previously discovered best monomers (PEG #8 and zwitterionic #40).

3.4. Membrane permeability versus selectivity (dynamic fouling)

In order to compare the performance for different gas separation polymer membranes, Robeson [41,42] developed a log–log plot of separation factor versus permeability similar to the classic plot of capacity versus selectivity for most separation processes. The data obtained from binary gas mixtures revealed an “upper bound”, above which nearly no data exists. Here, selectivity is measured as the ratio of the permeability of the small molecules (water and ions) to that of the less permeable BSA and is plotted as the function of the permeability of the modified and the control membrane (Fig. 6) [43]. A trade-off between selectivity and permeability is observed, as modified membranes with high selectivity displayed low permeability and *vice versa*. Membranes modified with monomers A3–A5 and A7 exhibited higher average permeability than the control membrane. Notably, modification with monomers A3 (3.05 LMH/kPa) and A7 (3.11 LMH/kPa) yielded membranes having higher average permeability than the previous PEG #8 (2.66 LMH/kPa) and zwitterionic #40 (2.58 LMH/kPa) modified membranes. The highest selectivity ($\Psi = 4.49 \pm 0.39$) and the lowest average permeability (0.61 LMH/kPa) were obtained from grafting with monomer A10. This is possibly due to the high electrostatic attraction between the A10 modified membrane surface with its positive polyelectrolyte and the negatively charged BSA at pH 7.4.

4. Conclusions

Combinatorial methods offer opportunities to expand the chemical space of monomers for protein-resistant (or anti-fouling) membrane surfaces. A series of amide monomers were synthesized from vinyl chloride and amine compounds with different functional groups. These newly synthesized amide monomers were used to modify commercial PES

membranes by high throughput atmospheric pressure plasma (HTP-APP). After challenging these membranes with BSA (static fouling), the PES membrane surfaces grafted with N-(3-hydroxypropyl)methacrylamide (A3), N-(4-hydroxybutyl)methacrylamide (A4), N-(4-hydroxybutyl) methacrylamide (A6), N-(3-methoxypropyl)methacrylamide (A7), N-(2-(dimethylamino)ethyl)-N-methylmethacrylamide (A8) and N-(2-(diethylamino)ethyl)-N-methylmethacrylamide (A9) were analyzed for protein resistance. A4 and A7 modified PES membranes exhibited both lower fouling and higher permeation flux when compared with the control membrane, and their performance was comparable with previously identified best monomers, PEG #8 and zwitterionic #40. After challenging membranes with a BSA filtration assay (dynamic fouling), A3 and A7 modified PES membranes exhibited the highest average permeability, and these membranes could be useful for BSA purification from blood (large industrial separation challenge). The A10 modified PES membrane showed the highest selectivity and could be useful for removing BSA from other permeable blood components. Structure–property analysis from the Hansen solubility parameters (HSPs) was predictive for experimental measurements and thus revealed the importance of surface– water interactions for reducing protein fouling.

Supplementary Material

Refer to Web version on PubMed Central for supplementary material.

Acknowledgments

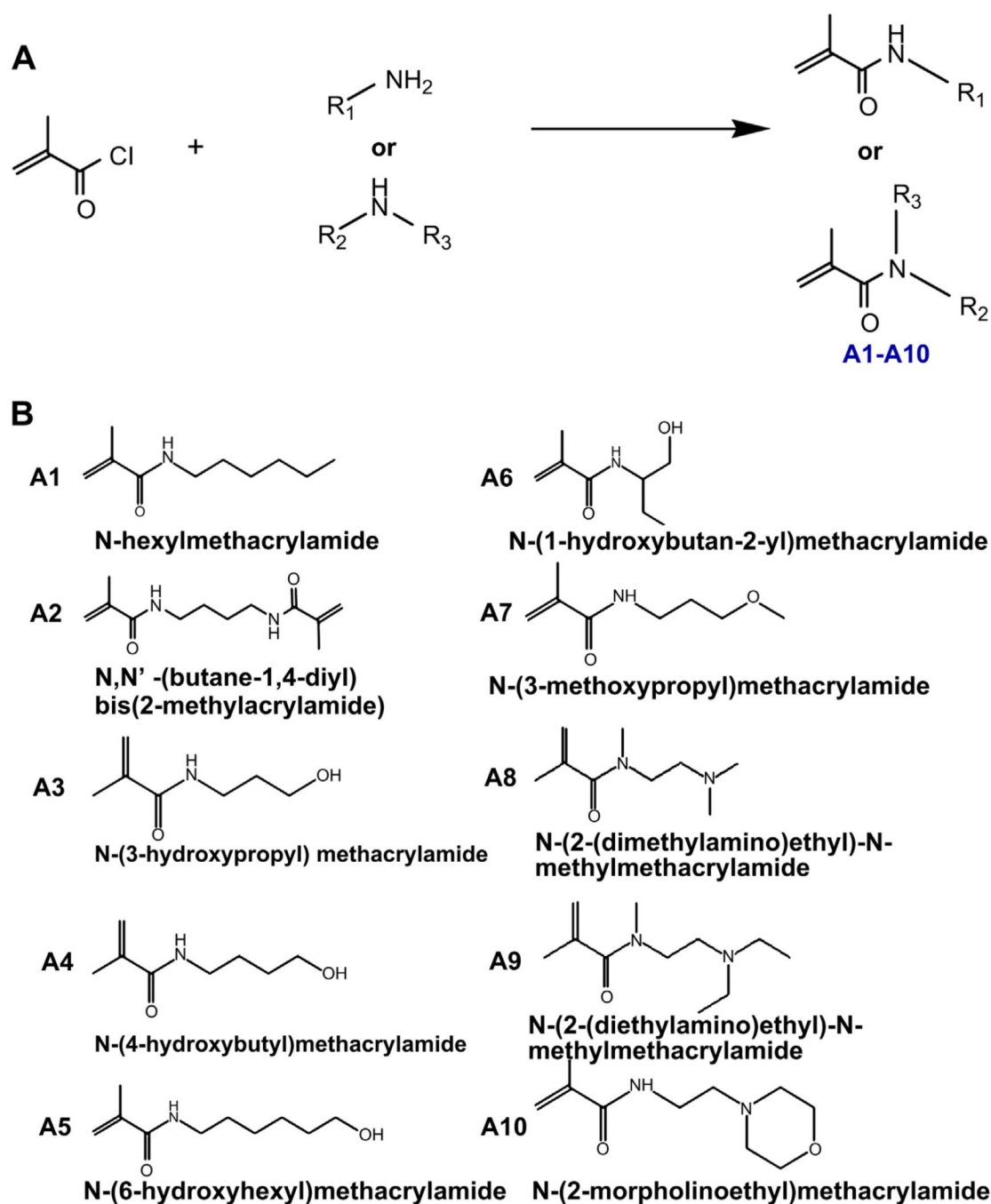
The authors acknowledge funding from the US Department of Energy (DOE DE-FG02-09ER16005 to GB), the National Science Foundation (NSF CBEF-0730449 to GB) and the National Institutes of Health (NIH DE016516 and DE013023 to RSL). Minghao Gu acknowledges a graduate fellowship from Howard P. Isermann. We also thank Seahorse Labware (Chicopee, MA) for the filter plates, Pall Corporation (Port Washington, NY) for PES membranes, Philip S. Yune for stimulating discussions and Mingyan Zhou for initiating and laying the foundation for the high throughput work.

References

1. Suk JS, Lai SK, Wang YY, Ensign LM, Zeitlin PL, Boylee MP, et al. The penetration of fresh undiluted sputum excreted by cystic fibrosis patients by non-adhesive polymer nanoparticles. *Biomaterials*. 2009; 30(13):2591–2597. [PubMed: 19176245]
2. Leonard, EF.; Turitto, VT.; Vroman, L. Blood in contact with natural and artificial surfaces. New York: New York Academy of Sciences: 1987.
3. Guell C, Davis RH. Membrane fouling during microfiltration of protein mixtures. *J Membr Sci*. 1996; 119(2):269–284.
4. Belfort G, Davis RH, Zydney AL. The behavior of suspensions and macromolecular solutions in crossflow microfiltration. *J Membr Sci*. 1994; 96(1–2):1–58.
5. Holmlin RE, Chen XX, Chapman RG, Takayama S, Whitesides GM. Zwitterionic SAMs that resist nonspecific adsorption of protein from aqueous buffer. *Langmuir*. 2001; 17(9):2841–2850.
6. Ostuni E, Chapman RG, Holmlin RE, Takayama S, Whitesides GM. A survey of structure-property relationships of surfaces that resist the adsorption of protein. *Langmuir*. 2001; 17(18):5605–5620.
7. Gao CL, Li GZ, Xue H, Yang W, Zhang FB, Jiang SY. Functionalizable and ultra-low fouling zwitterionic surfaces via adhesive mussel mimetic linkages. *Biomaterials*. 2010; 31(7):1486–1492. [PubMed: 19962753]
8. Li GZ, Cheng G, Xue H, Chen SF, Zhang FB, Jiang SY. Ultra low fouling zwitterionic polymers with a biomimetic adhesive group. *Biomaterials*. 2008; 29(35):4592–4597. [PubMed: 18819708]
9. Mi L, Bernards MT, Cheng G, Yu QM, Jiang SY. pH responsive properties of non-fouling mixed-charge polymer brushes based on quaternary amine and carboxylic acid monomers. *Biomaterials*. 2010; 31(10):2919–2925. [PubMed: 20045182]
10. Luk YY, Kato M, Mrksich M. Self-assembled monolayers of alkanethiolates presenting mannitol groups are inert to protein adsorption and cell attachment. *Langmuir*. 2000; 16(24):9604–9608.

11. Jeon SI, Andrade JD. Protein-surface interactions in the presence of polyethylene oxide: II. Effect of protein size. *J Colloid Interface Sci.* 1991; 142(1):159–166.
12. Murthy R, Shell CE, Grunlan MA. The influence of poly(ethylene oxide) grafting via siloxane tethers on protein adsorption. *Biomaterials.* 2009; 30(13):2433–2439. [PubMed: 19232435]
13. Crouzet C, Decker C, Marchal J. Characterization of primary oxidative degradation reactions in the course of the autooxidation of poly(oxyethylene)s at 25°C: study in aqueous solution with initiation by solvent irradiation. 8. Kinetic studies at pH between 1 and 13. *Makromol Chem.* 1976; 177(1):145–157.
14. Chen SF, Zheng J, Li LY, Jiang SY. Strong resistance of phosphorylcholine self-assembled monolayers to protein adsorption: insights into nonfouling properties of zwitterionic materials. *J Am Chem Soc.* 2005; 127(41):14473–14478. [PubMed: 16218643]
15. Ulbricht M, Matuschewski H, Oechel A, Hicke HG. Photo-induced graft polymerization surface modifications for the preparation of hydrophilic and low-protein-adsorbing ultrafiltration membranes. *J Membr Sci.* 1996; 115(1):31–47.
16. Gupta B, Plummer C, Bisson I, Frey P, Hilborn J. Plasma-induced graft polymerization of acrylic acid onto poly(ethylene terephthalate) films: characterization and human smooth muscle cell growth on grafted films. *Biomaterials.* 2002; 23(3):863–871. [PubMed: 11771705]
17. Gawish SM, Ramadan AM, Matthews SR, Bourham MA. Modification of PA6,6 by atmospheric plasma and grafting 2-hydroxy ethyl methacrylate (HEMA) to improve fabric properties. *Polym Plast Technol Eng.* 2008; 47(5):473–478.
18. Rovira-Bru M, Giralt F, Cohen Y. Protein adsorption onto zirconia modified with terminally grafted polyvinylpyrrolidone. *J Colloid Interface Sci.* 2001; 235(1):70–79. [PubMed: 11237444]
19. Yamagishi H, Crivello JV, Belfort G. Development of a novel photochemical technique for modifying poly (arylsulfone) ultrafiltration membranes. *J Membr Sci.* 1995; 105(3):237–247.
20. Taniguchi M, Belfort G. Low protein fouling synthetic membranes by UV-assisted surface grafting modification: varying monomer type. *J Membr Sci.* 2004; 231(1–2):147–157.
21. Ulbricht M, Belfort G. Surface modification of ultrafiltration membranes by low temperature plasma. I. Treatment of polyacrylonitrile. *J Appl Polym Sci.* 1995; 56(3):325–343.
22. Ulbricht M, Belfort G. Surface modification of ultrafiltration membranes by low temperature plasma. 2. Graft polymerization onto polyacrylonitrile and polysulfone. *J Membr Sci.* 1996; 111(2):193–215.
23. Belfer S, Fainshtain R, Purinson Y, Gilron J, Nystrom M, Manttari M. Modification of NF membrane properties by in situ redox initiated graft polymerization with hydrophilic monomers. *J Membr Sci.* 2004; 239(1):55–64.
24. Zhou MY, Liu HW, Kilduff JE, Langer R, Anderson DG, Belfort G. High throughput synthesis and screening of new protein resistant surfaces for membrane filtration. *AIChE J.* 2010; 56(7):1932–1945.
25. Zhou MY, Liu HW, Kilduff JE, Langer R, Anderson DG, Belfort G. High throughput discovery of new fouling-resistant surfaces. *J Mater Chem.* 2011; 21(3):693–704.
26. Gu MH, Kilduff JE, Belfort G. High throughput atmospheric pressure plasma-induced graft polymerization for identifying protein-resistant surfaces. *Biomaterials.* 2012; 33(5):1261–1270. [PubMed: 22123600]
27. Zhou MY, Liu HW, Kilduff JE, Langer R, Anderson DG, Belfort G. High-throughput membrane surface modification to control NOM fouling. *Environ Sci Technol.* 2009; 43(10):3865–3871. [PubMed: 19544900]
28. Maier WF, Kirsten G, Orschel M, Weiss PA, Holzwarth A, Klein J. Combinatorial chemistry of materials, polymers and catalysts. *ACS Symp Ser.* 2001; 814:1–21.
29. Yamashita DS, Dong XY, Oh HJ, Brook CS, Tomaszek TA, Szewczuk L, et al. Solid-phase synthesis of a combinatorial array of 1,3-bis(acylamino)-2-butanones, inhibitors of the cysteine proteases cathepsins K and L. *J Comb Chem.* 1999; 1(3):207–215. [PubMed: 10746010]
30. Raveglia LF, Vitali M, Artico M, Graziani D, Hay DWP, Luttmann MA, et al. Investigation of SAR requirements of SR 142801 through an indexed combinatorial library in solution. *Eur J Med Chem.* 1999; 34(10):825–835.

31. Lew A, Chamberlin AR. Blockers of human T cell Kv1.3 potassium channels using de novo ligand design and solid-phase parallel combinatorial chemistry. *Bioorg Med Chem Lett.* 1999; 9(23): 3267–3272. [PubMed: 10612582]
32. Anderson DG, Tweedie CA, Hossain N, Navarro SM, Brey DM, Van Vliet KJ, et al. A combinatorial library of photocrosslinkable and degradable materials. *Adv Mater.* 2006; 18(19): 2614–2618.
33. Pieracci J, Crivello JV, Belfort G. UV-assisted graft polymerization of N-vinyl-2-pyrrolidinone onto poly(ether sulfone) ultrafiltration membranes using selective UV wavelengths. *Chem Mater.* 2002; 14(1):256–265.
34. Hansen, CM. Hansen solubility parameters: a user's handbook. London: CRC Press; 2000.
35. Barton, A. CRC handbook of solubility parameters and other cohesion parameters. 2nd ed.. London: CRC Press; 1991.
36. Jeon SI, Lee JH, Andrade JD, Degennes PG. Protein-surface interactions in the presence of polyethylene oxide: I. Simplified theory. *J Colloid Interface Sci.* 1991; 142(1):149–158.
37. Pertsin AJ, Grunze M. Computer simulation of water near the surface of oligo(ethylene glycol)-terminated alkanethiol self-assembled monolayers. *Langmuir.* 2000; 16(23):8829–8841.
38. Hower JC, He Y, Bernards MT, Jiang SY. Understanding the nonfouling mechanism of surfaces through molecular simulations of sugar-based self-assembled monolayers. *J Chem Phys.* 2006; 125(21)
39. Hower JC, Bernards MT, Chen SF, Tsao HK, Sheng YJ, Jiang SY. Hydration of “nonfouling” functional groups. *J Phys Chem B.* 2009; 113(1):197–201. [PubMed: 19072165]
40. Harder P, Grunze M, Dahint R, Whitesides GM, Laibinis PE. Molecular conformation in oligo(ethylene glycol)-terminated self-assembled mono-layers on gold and silver surfaces determines their ability to resist protein adsorption. *J Phys Chem B.* 1998; 102(2):426–436.
41. Robeson LM. Polymer blends in membrane transport processes. *Ind Eng Chem Res.* 2010; 49(23): 11859–11865.
42. Robeson L. Correlation of separation factor versus permeability for polymeric membranes. *J Membr Sci.* 1991; 62(2):165–185.
43. Mehta A, Zydny AL. Permeability and selectivity analysis for ultrafiltration membranes. *J Membr Sci.* 2005; 249(1–2):245–249.

**Fig. 1.**

(A) Synthesis of amide monomers by reactions of methacryloyl chloride with amines, and (B) list of names and chemical structures of the synthesized amide monomer, A1–A10. A1 is an internal control as it has not hydroxyl group at the terminus; A3–A5 increased in length by one carbon group; A6 is a branched version of A4; A7 is a methyl-terminated PEG; A8–A10 are terminated with tertiary amines. A10 is slightly positive.

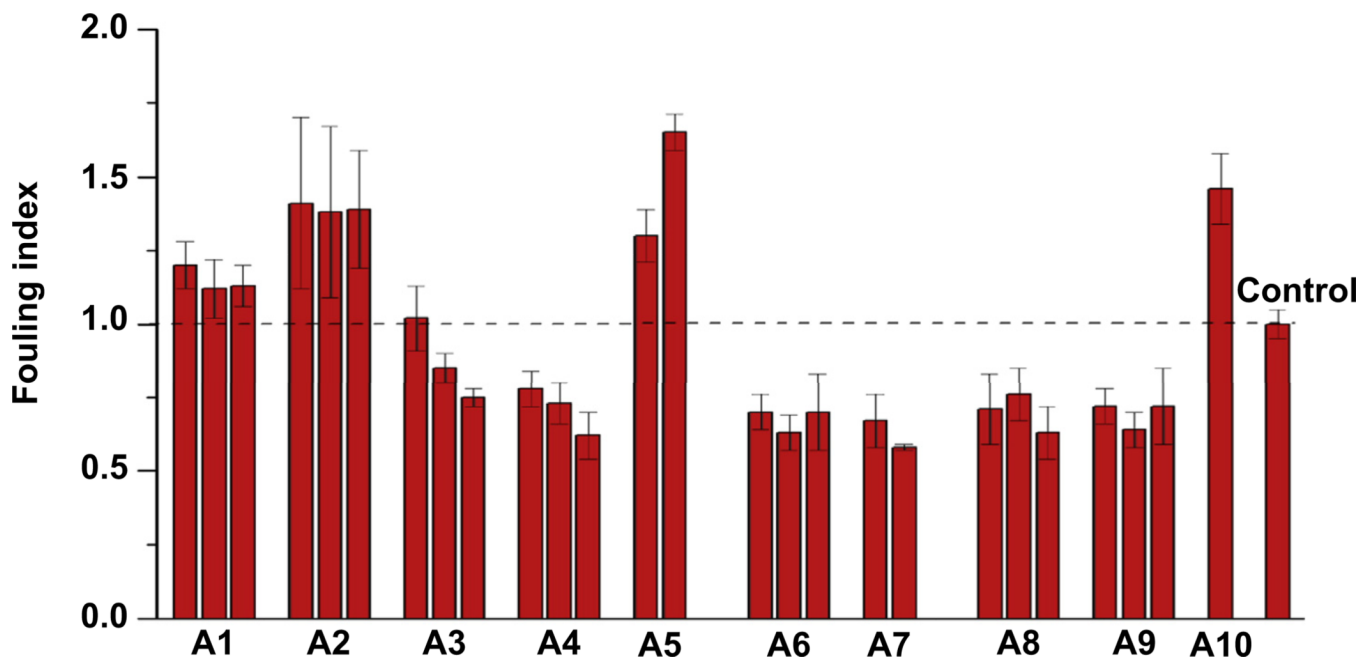


Fig. 2.

Fouling index or \mathcal{R} values of PES membranes grafted with amide monomer A1–A10 by HTP-APP after 1 mg/mL BSA adsorption for 44 h at $T = 22 \pm 1$ °C and pH 7.4. Ethanol/water (20/80 wt%/wt%) was used as the solvent for A1 and A5, and ethanol was used as the solvent for A2. \mathcal{R} values for A1–A4, A6, A8 and A9 were obtained with 0.1 M, 0.2 M and 0.3 M monomer solution (from left to right for each monomer). \mathcal{R} values of 0.3 M A5 and 0.3 M A7, and 0.2 M and 0.3 M A10 were not shown due to the very low permeation after adsorption (difficult to measure). Each data point was obtained in quadruplicate.

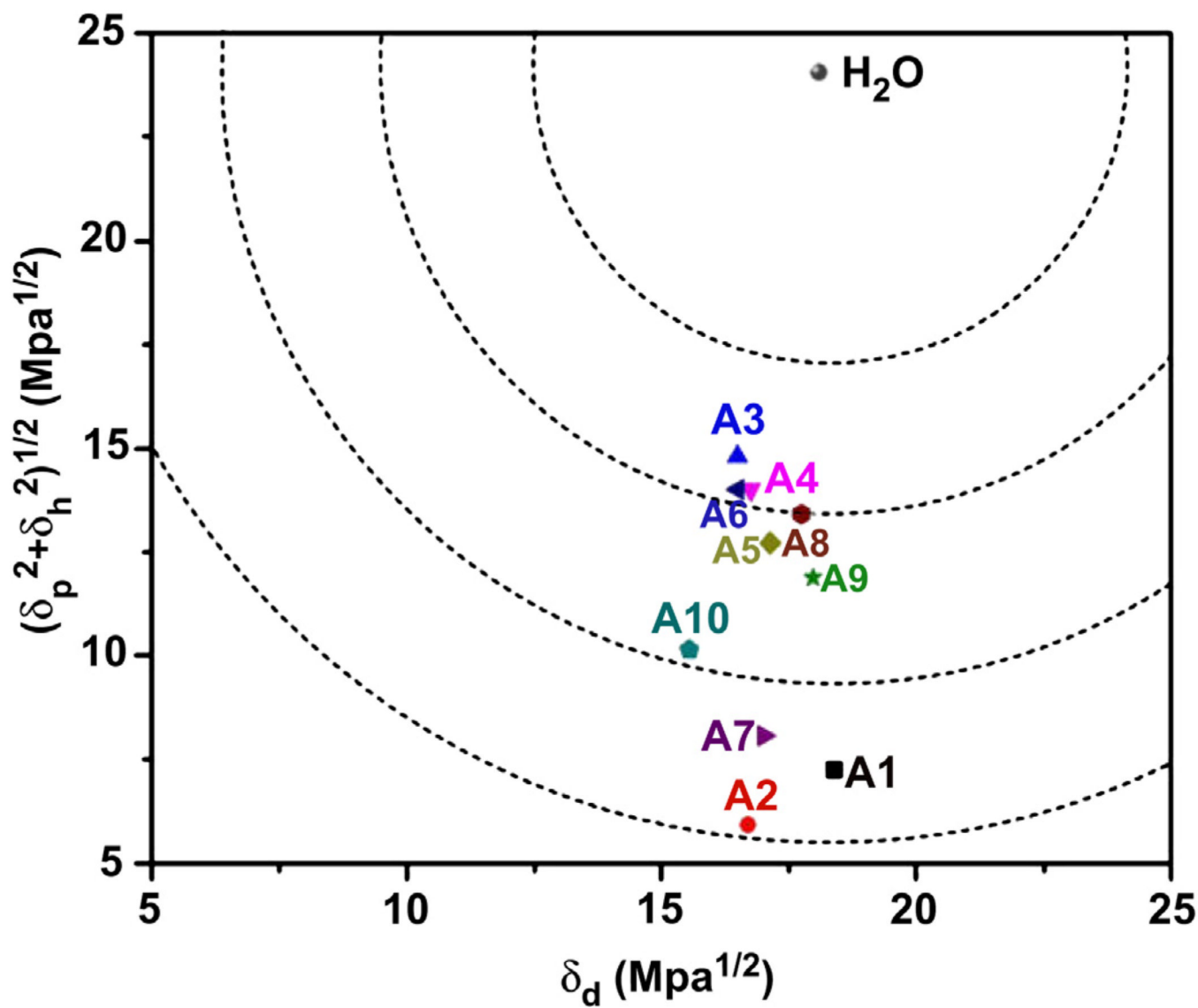


Fig. 3.

Hansen solubility parameters (HSPs) of δ_d versus $(\delta_p^2 + \delta_h^2)^{1/2}$ of amide monomers and water.

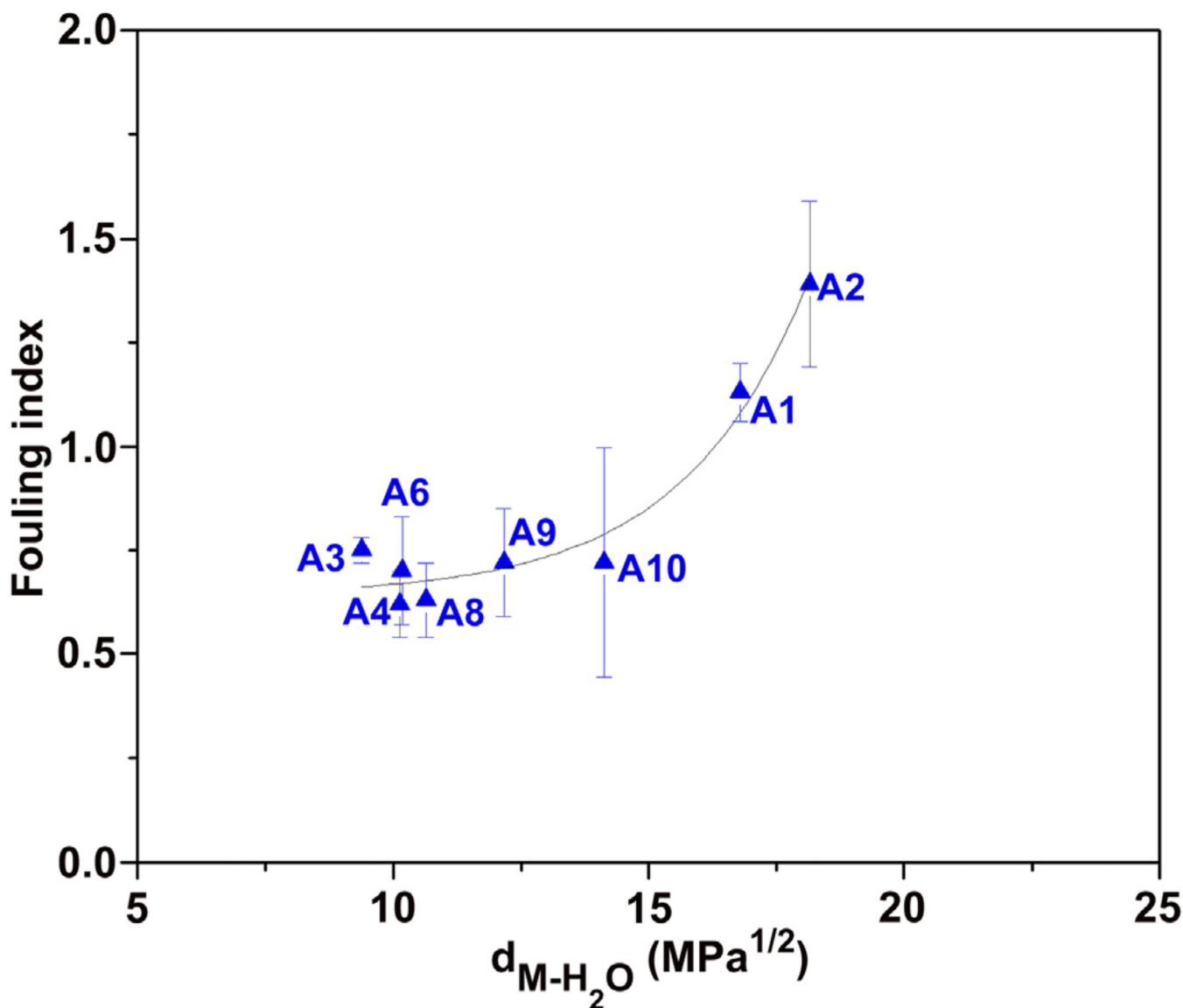


Fig. 4.

Fouling index versus distance, d_{M-H_2O} , from a monomer point to the water point. Fouling index was obtained with 0.3 M monomer concentration (Fig. 2). Here,

$$d_{M-H_2O} = \left\{ \left[(\delta_{p,M}^2 + \delta_{h,M}^2)^{0.5} - (\delta_{p,H_2O}^2 + \delta_{h,H_2O}^2)^{0.5} \right]^2 (\delta_{d,M} - \delta_{d,H_2O})^2 \right\}^{0.5}$$
, where, $\delta_{d,M}$, $\delta_{p,M}$ and $\delta_{h,M}$ are the non-polar, polar and hydrogen bonding components of a monomer's HSP, respectively; δ_{d,H_2O} , δ_{p,H_2O} and δ_{h,H_2O} are the non-polar, polar and hydrogen bonding components of water's HSP, respectively. Fouling index versus d_{M-H_2O} was fit with an exponential curve: $y = 0.64 + 4.73 \cdot 10^{-4} \cdot e^{(x/2.46)}$, $R^2 = 0.96$.

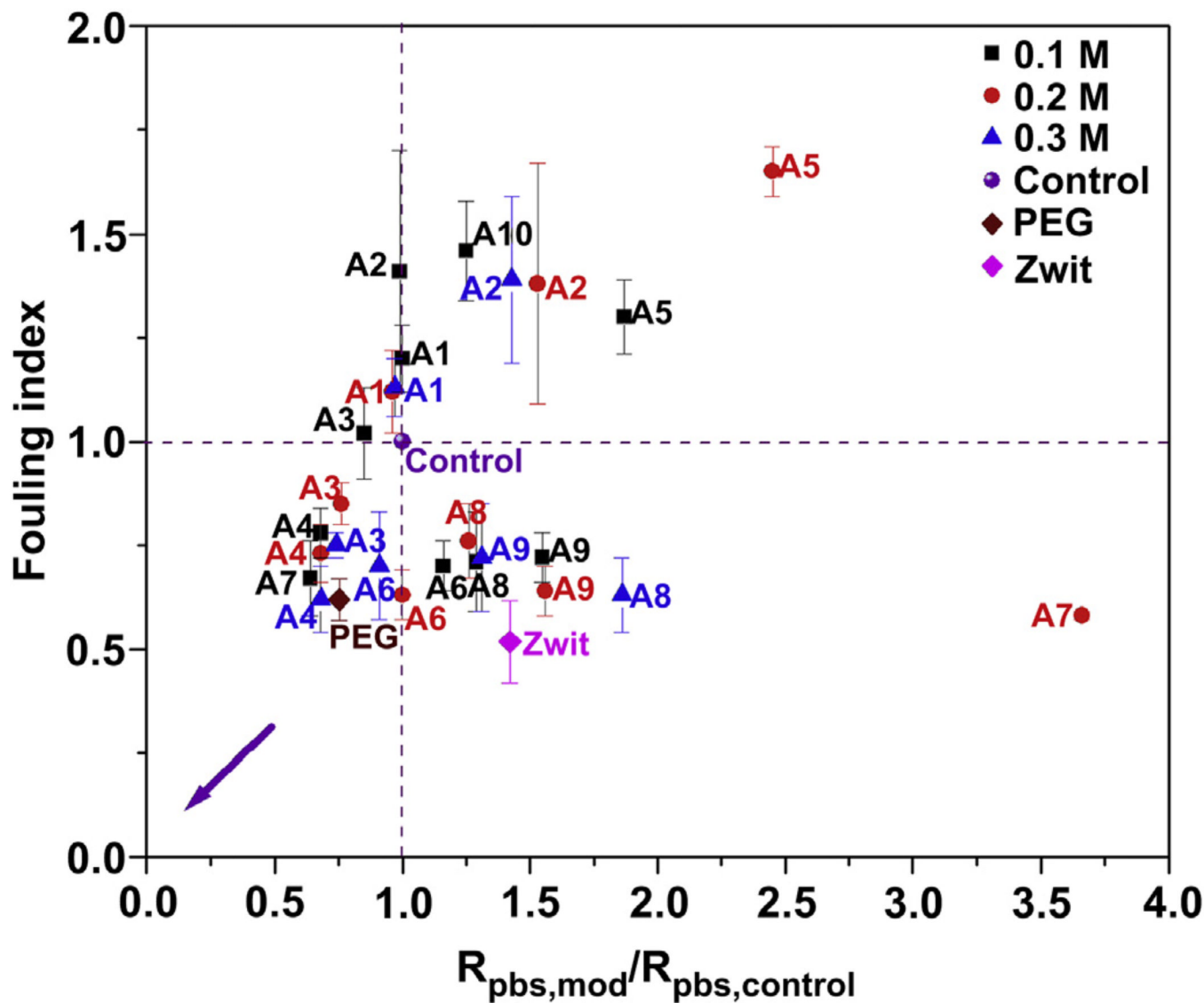


Fig. 5. Fouling index versus ratio of inverse permeation flux of the modified PES membranes to the control membrane as measured by HTP-APP. 1 mg/mL BSA adsorption for 44 h at $T = 22 \pm 1$ °C and pH 7.4 and filtration at TMP = 68 kPa, $T = 22 \pm 1$ °C and pH 7.4. Data for an unmodified membrane (control), a PEG (#8) and a zwitterionic (#40) modified membrane are also included. Each data point was obtained in quadruplicate.

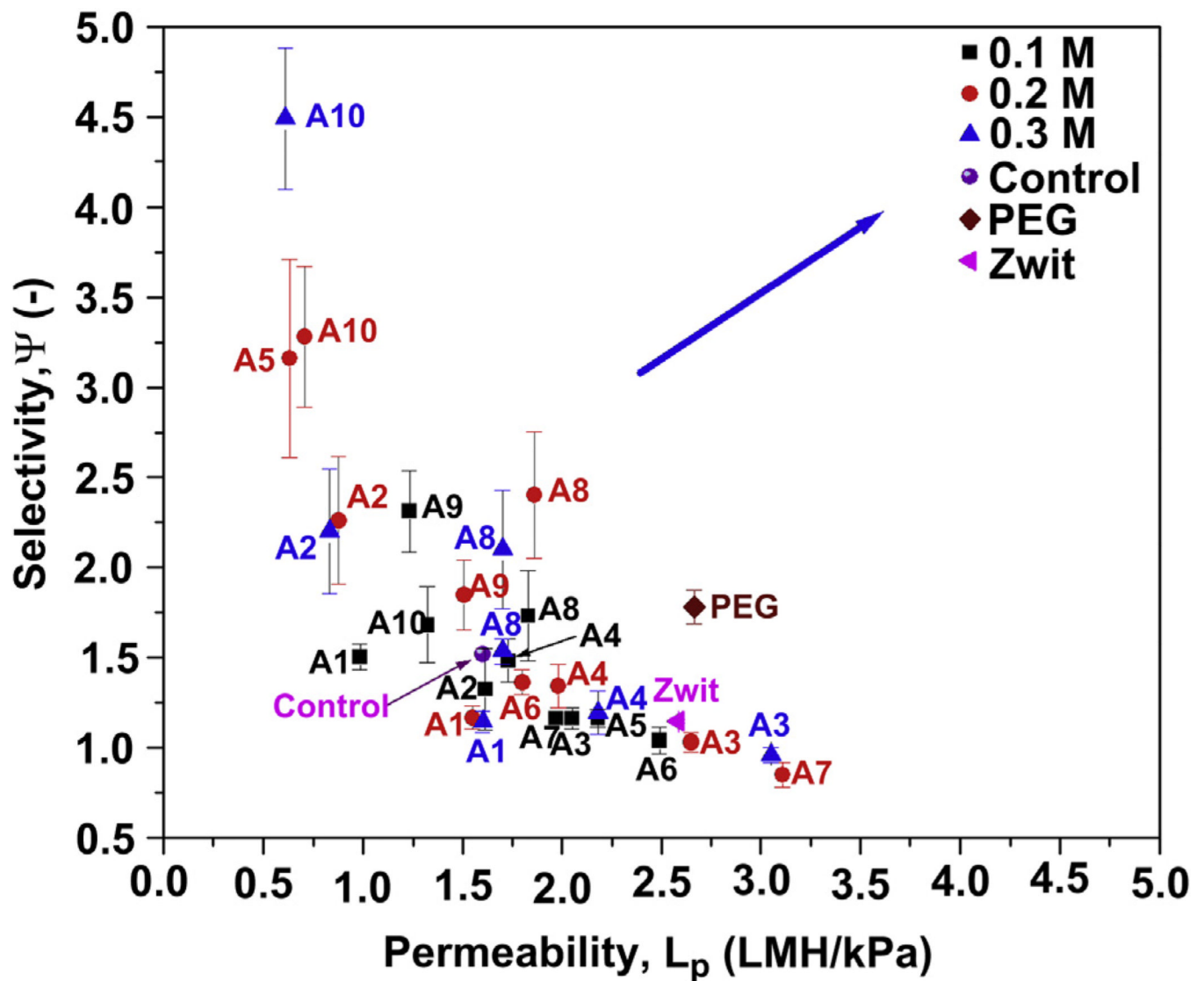


Fig. 6. Selectivity versus permeability plot for the amide modified PES membranes and the control membrane by HTP-APP after 1 mg/mL BSA solution filtration at TMP = 68 kPa, $T = 22 \pm 1$ °C and pH 7.4. Data for an unmodified membrane (control), a PEG (#8) and a zwitterionic (#40) modified membrane are also included. Each data point was obtained in quadruplicate.